https://doi.org/10.31436/iiumej.v27i3.4618

A TRIZ-Based Conceptual Design of an Automatic Footrest Stand to Enhance Lateral Stability of the Flexible Unicycle Prototype During Mounting and Dismounting

NOORHIDAYAH RAMLI, MUHAMMAD AZIM AZIZI*, MUHAMMAD AMIN AZMAN, NURAINI AB AZIZ

Department of Mechanical and Manufacturing Engineering, Faculty of Engineering, Universiti Putra Malaysia, 43400, Serdang, Selangor, Malaysia

**Corresponding author: muhdazim@upm.edu.my*

(Received: 21 July 2026; Accepted: 18 August 2026; Published online: 11 September 2026)

ABSTRACT: This paper outlines the conceptual design of a support mechanism developed to improve the lateral stability of electric unicycles (EUCs), specifically the existing Flexi-UC design, during mounting and dismounting without compromising its compact and lightweight features. The study highlights the application of the Theory of Inventive Problem Solving (TRIZ), which enables the mechanism concept to be developed systematically according to the specified design requirements. Several TRIZ tools were applied, namely Functional Analysis, Cause-and-Effect Chain Analysis, Engineering Contradiction, and Physical Contradiction. As a result, Inventive Principle 7, the Nested Doll Principle, was selected and applied in developing the automatic stand design. Finite Element Analysis (FEA) was conducted to verify the automatic stand's structural reliability. The results showed that the structure could safely support a maximum rider mass of 100 kg. The corresponding load produced a maximum von Mises stress of 66.723 MPa and a maximum deformation of 0.363 mm, both of which are below the allowable limits for mild steel. In addition, theoretical stability analysis indicates that the critical angle increases from −6.01° without the stand to 10.9° with the automatic stand deployed, providing a significantly wider stability margin. Overall, the results demonstrate that the TRIZ-based approach is an effective method for generating conceptual designs that enhance the lateral stability of the Flexi-UC during mounting and dismounting.

ABSTRAK: Kajian ini menekankan aplikasi Teori Penyelesaian Masalah Inventif (TRIZ), membolehkan konsep mekanisme dibangunkan secara sistematik dalam memenuhi keperluan reka bentuk yang ditetapkan. Beberapa kaedah TRIZ telah digunakan iaitu Analisis Fungsi, Analisis Rantaian Sebab dan Akibat, Percanggahan Kejuruteraan dan Percanggahan Fizikal. Hasilnya, Prinsip Rekacipta 7 iaitu Nested Doll telah terpilih dan rekabentuk tongkat automatik telah digunakan. Analisis Unsur Terhingga (FEA) telah dijalankan bagi mengesahkan kebolehpercayaan struktur tongkat automatik tersebut, dan hasil analisis menunjukkan bahawa struktur tersebut mampu menampung beban penunggang maksimum seberat 100 kg dengan selamat. Beban tersebut menghasilkan tegasan Von Mises maksimum sebanyak 66.723 MPa dan ubah bentuk maksimum sebanyak 0.363 mm, kedua-duanya berada di bawah had yang dibenarkan bagi bahan keluli ringan. Selain itu, analisis kestabilan secara teori menunjukkan bahawa sudut kecondongan kritikal meningkat daripada −6.01° tanpa sokongan tambahan kepada 10.9° dengan penggunaan tongkat automatik, sekaligus memberikan margin kestabilan yang lebih besar. Secara keseluruhan, dapatan kajian menunjukkan bahawa pendekatan berasaskan TRIZ merupakan kaedah berkesan dalam menghasilkan reka bentuk konseptual yang dapat meningkatkan kestabilan lateral Flexi-UC semasa proses naik dan turun.

KEYWORDS: *TRIZ, Lateral Stability, Micromobility, Electric Unicycle, Finite Element Analysis.*

https://doi.org/10.31436/iiumej.v27i3.4618

1. INTRODUCTION

Conceptual design is a process in which possible design options are defined early in the design phase after identifying product requirements and specifications. This step is crucial as it establishes the foundation of the final product and has a significant bearing on the overall performance and functionality [1]. Traditional conceptual design methods are often based on brainstorming to generate intuitive ideas or on logical methods that apply structured procedures [2]. TRIZ offers a more analytical and systematic method compared to these approaches, enabling the creation of innovative yet realistic solutions [3]. Unlike conventional brainstorming methods, TRIZ uses structured tools, including the contradiction matrix, separation principles, and functional analysis. Building on these strengths, this study uses TRIZ to conceptually design an automatic footrest stand system. This system aims to enhance the lateral stability of electric unicycles (EUCs) during the critical phases of mounting and dismounting.

Recent studies have demonstrated TRIZ's applicability in micromobility design. For instance, in 2023, a systematic review noted the effective use of TRIZ in designing e-scooters and e-bikes to enhance safety while reducing weight and size [4]. Moreover, case studies in 2023 and 2024 have shown how the contradiction matrix and functional analysis can be used to improve the design of foldable scooters and their ergonomics [5]. More advanced methods have also been adopted in the development of lightweight vehicles, where efforts have focused on computer-aided TRIZ techniques and systematic prototyping to achieve a balance between structural integrity and lightness [6]. While TRIZ has proven effective for multi-wheel micromobility systems, its application to self-balancing single-wheel vehicles remains largely unexplored in the literature. This conceptual stage provides the basis for subsequent structural analysis and prototype development, contributing to a more balanced and user-friendly electric unicycle. Among micromobility systems, the EUC is one of the most compact yet most challenging platforms to balance.

An EUC is a small personal electric motorized vehicle with a single wheel, which is driven by an electric motor and regulated by an inbuilt gyroscope that reacts to changes in the rider's body angle and position [6] . When the rider leans forward, the EUC moves forward, and when the rider leans backward, it reverses. EUCs have integrated control mechanisms that include both gyroscopes and accelerometers, which enable them to maintain balance in both the forward and backward directions. The EUC consists of a frame with the battery, motor, electronic controller, and a central wheel.

Despite continuous technological advances, most commercial EUCs continue to experience poor lateral balance, particularly at low speeds or when at rest [6]. Similar to a bicycle, when the device's forward speed is reduced, the stabilizing effect of forward momentum and gyroscopic action diminishes, increasing susceptibility to lateral instability at low speeds. Novice riders may experience difficulty placing their feet on the footrests, and any minor imbalance may cause the EUC to lean over. The rider's weight transfer during dismounting may disrupt the gyroscopic system's response, resulting in unintended motion that may cause imbalance or a fall [7]. This sudden action may reduce novice riders' confidence and perception of safety. Lateral stability is therefore critically important, especially during starting and stopping, when riders are at the greatest risk of losing balance [7]. Previous studies have investigated rider balancing and EUC dynamics during different riding maneuvers [8]. However, stability during mounting and dismounting remains an important issue that requires further consideration.

The development of the Flexible Electric Unicycle, known as Flexi-UC [9] focused on improving lateral stability during riding, cornering, and low-speed operation. As illustrated in

Figure 1, both sides of the main wheel were equipped with small auxiliary wheels to provide lateral support, helping riders stay balanced during riding. This prototype showed that lateral instability could be minimized by adding compact support elements without sacrificing the EUC's portability.

Figure 1. Flexi-UC with 2 auxiliary wheels on both sides

However, the Flexi-UC does not assist the rider during mounting and dismounting, when lateral instability still exists. This gap motivated the present study to develop an additional lateral-support mechanism through a TRIZ-based conceptual design. This systematic approach is intended to generate a mechanism that provides lateral support without compromising the compactness and portability of the Flexi-UC, specifically during mounting and dismounting. The findings are limited to the geometry, configuration, and operating conditions of the Flexi-UC used in this study and should not be generalized to other electric unicycle configurations without further validation.

Table 1. The comparison of the Flexi-UC with 2 existing electric unicycles on the market

Parameter	**Original Flexi-UC**	**InMotion V11Y [10]**	**Airwheel Q3 [11]**
Dimensions (mm)	690 x 500 x 450	500 × 180 × 744	518 × 408 × 200
Wheel/tire configuration	1 main + 2 side wheels	Single 18 × 3 in tire	Two coaxial 14 in wheels
Stabilization mechanism	Electronic self-balancing + Flexible auxiliary wheels	Electronic self-balancing + suspension	Electronic self-balancing + passive lateral support from twin wheels
Lateral support during mounting/dismounting	Side-wheels ground support	Rider dependent	Twin-wheel ground contact
Advantage	Improved lateral stability during riding/cornering	Suspension and ride comfort	Wider contact area provides improved lateral stability
Limitation	Insufficient support during mounting/dismounting	Requires rider lateral balance	Fixed twin-wheel configuration increases width and cannot retract during riding

Table 1 shows that the three designs use different approaches to improve stability and riding performance. The Flexi-UC incorporates side wheels to improve lateral stability during riding, while the commercial models mainly rely on electronic self-balancing and suspension systems. However, lateral stability during mounting and dismounting remains dependent on adequate ground support or rider control. This limitation provides the basis for developing an additional support mechanism for the existing Flexi-UC. Therefore, this study proposes a

https://doi.org/10.31436/iiumej.v27i3.4618

TRIZ-based automatic footrest stand to improve the Flexi-UC's lateral stability during mounting and dismounting.

The objective of this paper is to develop and evaluate a conceptual support mechanism to improve the lateral stability of a Flexi-UC, particularly during mounting and dismounting. The study applies a TRIZ-based approach to identify the root causes of instability and to guide the development of the proposed design. In addition, analytical stability analysis and finite element analysis are carried out to assess the effectiveness and structural reliability of the proposed mechanism.

2. METHODOLOGY

The methodology will be divided into four stages to develop and evaluate the proposed design. Each stage will address a specific aspect of the research, where Stage 1 will focus on problem identification and conceptual design using the TRIZ method, Stage 2 will involve theoretical stability analysis using analytical equations, Stage 3 will cover Finite Element Analysis (FEA), focusing on structural analysis and optimization, and Stage 4 will involve the fabrication and integration of the proposed conceptual design into the Flexi-UC.

2.1. Problem Analysis and Conceptual Design Using the TRIZ Method.

TRIZ is a systematic method that helps identify design conflicts and generate suitable solution ideas without restricting how the mechanism should be developed. However, TRIZ does not consider the mechanical feasibility of the proposed conceptual solutions. FEA, by contrast, enables numerical evaluation of structural behavior under applied loading conditions. Thus, TRIZ and FEA are complementary: TRIZ drives conceptual innovation and guides functional and mechanism-level design, while FEA verifies structural integrity, quantifies performance, and supports further refinement of the design parameters. In this work, TRIZ was applied to develop the deployable lateral support concept, which was subsequently evaluated using FEA to assess and optimize the design geometry and ensure that the proposed inventive solution has sufficient strength and stiffness during operation.

The TRIZ problem-solving map shown in Figure 2 is adapted from the approach described in [12]. It outlines a sequence of steps to investigate a technical problem and develop innovative solutions. The diagram indicates that the process begins with defining the original problem, followed by functional analysis and Cause and Effect Chain Analysis (CECA), which help identify the root causes of the harmful function, and then proceeds through systematic analytical and creative steps toward identifying an appropriate solution. Rather than following a fixed linear sequence, TRIZ allows selective use of each step, depending on its relevance to the engineering problem [13]. Some tools may also be unnecessary or redundant in certain projects [13].

The current design of Flexi-UC is compact, with a small support base defined by the two auxiliary wheels, making it laterally unstable during mounting and dismounting. Specifically, the footrest lacks structural support beneath it to counteract the moment generated by the rider’s weight, causing the unicycle to topple. This mechanical limitation was evident in the current Flexi-UC prototype, which, although effective in enhancing lateral stability during motion via auxiliary wheels, still requires improvement during mounting and dismounting. This functional weakness defined the critical design problem of the present work.

To address this, the problem was initially identified and analyzed through functional analysis and Cause and Effect Chain Analysis. These analyses revealed the primary weakness in lateral stability and the competing needs of the footrest system. Based on these findings, the

TRIZ tools, namely Engineering Contradiction (EC), Physical Contradiction (PC), and Function Modeling (FM), were applied to identify the most feasible solution. Through this process, a paradox was identified: the stand must be deployed to provide support but retracted during riding to avoid compromising the vehicle's compactness. This contradiction was addressed using the TRIZ separation principles to ensure that both conditions could be achieved without impeding performance.

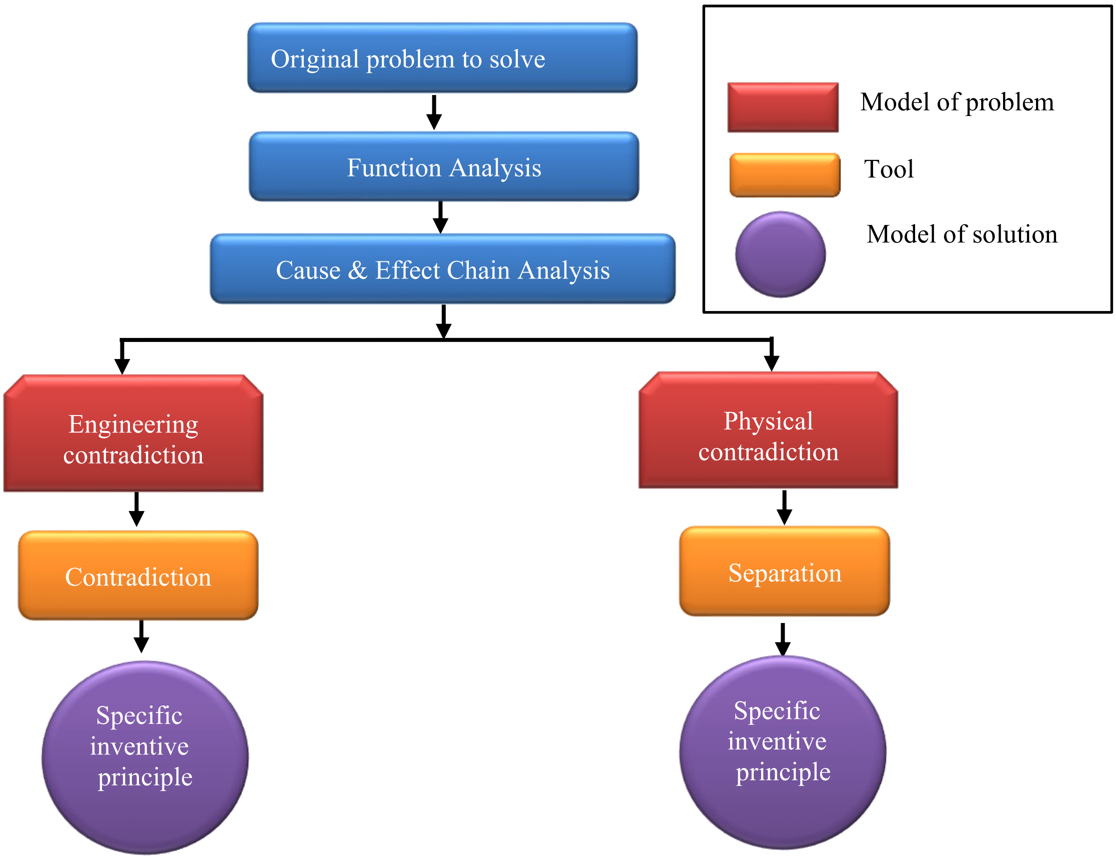

Figure 2. TRIZ problem-solving map adapted from [12].

2.1.1. Function Analysis

The Function Analysis (FA) process has three distinct steps: component analysis, interaction analysis, and functional analysis. Component analysis identifies the system's components and their corresponding functions. Interaction analysis focuses on how the system components affect each other, including both beneficial and harmful interactions. Functional analysis further assesses these interactions to determine whether the functions support or hinder overall system performance [13]. This analysis used the existing Flexi-UC prototype as the reference model and identified the sources of lateral instability.

In the first step, known as the component analysis phase, the Flexi-UC system is defined by identifying its system boundary and the elements that interact with it. As summarized in Table 2, the system consists of the left and right footrests, the unicycle frame, main wheel, the support wheel, the motor, and the electronic board. The supersystem includes the rider, the ground surface, and the surrounding environment, which provide the external loads and contact conditions that affect the system's stability and operation. By considering both the system and supersystem components, the functional analysis ensures that all relevant interactions influencing stability are identified, reducing the likelihood of overlooking critical factors during the design process.

Table 2. The component analysis of the engineering system and its supersystem

Description of engineering system	Components of the system	Components of the supersystem
Engineering system for Flexi-UC	Left footrest Right footrest Unicycle frame Main wheel 2 support wheels Motor Electronic board	Rider's foot, ground, weather, road condition, weight of the rider.

Meanwhile, Table 3 presents the second step: component interaction analysis. The plus sign (+) is used to describe the existence of a functional interaction between two components, whereas the minus sign (-) is used to describe the non-existence of direct interaction.

Table 3. Component interaction analysis

Components	x-axis								
	Rider	Right Footrest	Left Footrest	Unicycle Frame	Electronic Board	Motor	Main wheel	2 support wheels	Ground
Rider	-								
Right footrest	+	-							
Left Footrest	+		-						
Unicycle frame		+	+	-					
Electronic board				+	-				
Motor					+	-			
Main wheel				+		+	-		
2 support wheels				+				-	
Ground							+	+	-

The rider contacts the footrests, which are the primary interfaces for transmitting weight and balance input to the unicycle. The left and right footrests are mechanically connected to the unicycle frame, the primary load-bearing structure that integrates the motor, main wheel, electronic board, and support wheels. The main wheel provides direct contact with the ground, enabling propulsion and transferring vertical loads. The support wheels connect the unicycle frame to the ground and provide additional lateral contact in the Flexi-UC baseline design. Elements of the supersystem, including the rider's foot, ground, road conditions, weather, and the rider's weight, interact with the engineering system and influence its stability behavior. Overall, the component analysis identifies the principal load-transfer paths and control interactions within the system, thereby facilitating the identification of missing or weak interactions that contribute to lateral instability during mounting and dismounting.

The earlier design of Flexi-UC [9] lacks a support mechanism to assist with lateral balance during mounting and dismounting, and this aspect has received limited attention in previous studies because riders often rely on external support, such as a wall or support handle, when mounting and dismounting the unicycle. However, Nicholas [14] stated that mastering the EUC, particularly for beginners, is challenging because it requires precise control and balance to mount and dismount successfully.

The final step in the function analysis process is functional analysis, which evaluates the functions resulting from interactions between system and supersystem components to identify effective functions and potential problem areas. Figure 3 shows the functional analysis of the Flexi-UC system, illustrating the footrest's interaction with the internal subsystems and the external rider–environment interface. The diagrams use different arrow and line types to categorize the system's main functions, auxiliary functions, interrelations among system elements, and possible negative effects. The right footrest and the rider's foot are positioned lower during lateral imbalance, as shown in the baseline scenario in Figure 3, causing an uneven distribution of the rider's weight. As stability decreases, the load shifts increasingly to one side, reducing the footrest's ability to act as an effective stabilizing surface. This increases the likelihood that the system will tip sideways.

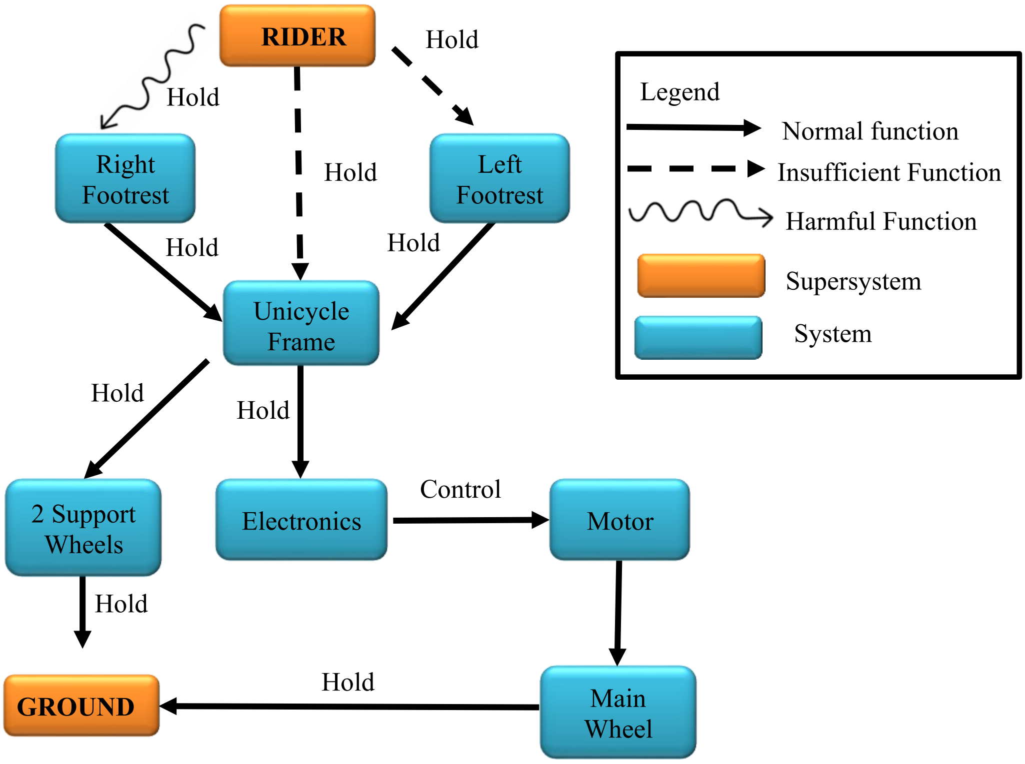

Figure 3. Function analysis of the system before improvement

Focusing on the mounting and dismounting phase, Figure 3 shows the functional model of the Flexi-UC before implementing the stability enhancement mechanism. In this configuration, the rider's balance acts as the primary stabilizing factor, and the left and right footrests serve only as platforms for the rider's feet. In the diagram, the rider's right foot is loosely placed on the right footrest, while the left foot remains on the ground. This instability worsens in the next step, when the rider attempts to quickly place the left foot on the left footrest. At this stage, a novice rider may experience significant lateral instability, which can result in unsuccessful mounting or even a fall. The electronic board, gyroscope, motor, and main wheel are integrated into the unicycle frame, enabling forward and backward movement through the control system; however, these subsystems do not directly contribute to lateral stabilization during mounting.

2.1.2. Cause and Effect Chain Analysis (CECA)

One major TRIZ tool is Cause and Effect Chain Analysis (CECA), which identifies and visualizes the root causes of an identified problem. It starts with defining the system's undesired function and then repeatedly asks "why" to identify further causal connections [15]. This method helps uncover underlying contradictions and root causes. CECA is commonly applied alongside functional and system analyses, serving as a transition between identifying the problem and developing creative TRIZ solutions.

2.1.3. Engineering contradiction

Engineering Contradiction (EC) was applied after CECA to identify conflicting design requirements, where improving one parameter may worsen another. The identified parameters were mapped into the TRIZ contradiction matrix, which consists of 39 engineering parameters and 40 inventive principles, to generate relevant inventive principles [13]. The generated principles were then evaluated against the design requirements to identify the most suitable principle for the proposed mechanism.

2.1.4. Physical Contradiction

Physical Contradiction (PC) was applied to address opposite requirements of the same design parameter, particularly the need for a large ground-contact area for stability and a small area for compactness. The four TRIZ separation principles, namely Separation in Time, Separation in Space, Separation upon Condition, and Separation between Whole and Parts, were evaluated based on their relevance to the design problem [13]. The most applicable separation principles were then used to determine when the proposed support mechanism should be deployed or retracted.

2.2. Stability analysis based on analytical equations.

The second stage will use analytical equations to evaluate the support stand's impact on stability. Two main indicators were considered: critical angle and stability margin.

2.2.1. Critical angle

The critical angle is the inclination at which a ground-contact system loses static stability. This occurs when the stability margin becomes zero, and the vertical projection of the center of gravity reaches the boundary of the support area. Beyond this angle, the system will tip over, as reported in [16]. The critical tilt angle is calculated based on geometric considerations of static stability, where the vertical projection of the combined center of mass reaches the edge of the support base. In this study, we define the critical angle using the same geometric principle as the rider tilt angle reported by Mungan [17], where the angle is obtained from the inverse tangent of the ratio of the horizontal offset of the center of mass to its vertical height.

$$\theta_{\text{critital}} = \tan^{-1}\left(\frac{\text{Horizontal offset}}{\text{Vertical offset}}\right) \tag{1}$$

For clarity, the horizontal offset term in the present work corresponds to the horizontal coordinate difference reported in prior unicycle tilt studies, in which b is half of the effective width of support, x is the horizontal deflection of the center of gravity (CoG), while h_{eff} representing the vertical offset, and both describe the horizontal distance between the center of mass and the reference support point; the formula is simplified to be:

$$\theta_{\text{critital}} = \tan^{-1}\left(\frac{b-\chi_{\text{eff}}}{h_{\text{eff}}}\right) \tag{2}$$

The system requires accurate geometric parameters for computation; thus, the unicycle–rider system was modeled in CATIA. The simulation provided CoG coordinates under static conditions, which were then applied in the stability equations to compare the existing Flexi-UC with the proposed design incorporating the stand.

2.2.2. Stability margin

In this study, stability is determined by evaluating how the object's center of gravity (CoG) relates to the support area on the ground. The system is considered stable when the projected CoG lies within the support polygon, defined by the points of contact between the ground and the system. When the projection falls outside the support limit, the system becomes unstable [16]. Thus, the stability margin is the distance between the projected center of gravity (CoG) and the nearest support edge. The critical tipping point occurs when this distance is zero [16].

The stability margin provides a convenient measure of how far the center of gravity (CoG) projection remains within the support polygon during a lateral lean. While Morales et al. [18] formulated the stability margin for a general polygon geometry, the present study adopts an expression adapted to the Flexi-UC configuration, where lateral stability is governed primarily by a single effective support boundary. The lean angle (φ) refers to the instantaneous tilt of the unicycle–rider system away from the vertical, representing the degree of leaning at a given moment. In its general form, the margin is expressed as $SM = b - d_{CoG}$, where b is the horizontal distance from the system's centerline to the edge of the support base, and d_{CoG} is the lateral displacement of the projected CoG. A positive value indicates stable equilibrium, whereas a negative value indicates tipping.

For the present unicycle application, the CoG projection displacement can be approximated as:

$$d_{\text{CoGProjection}} = \chi_{\text{eff}} + h.\tan(\varphi) \tag{3}$$

where h is the unicycle CoG height and φ represents the effective instantaneous lean angle. Substituting this relation yields the simplified expression:

$$SM = b - (\chi_{\text{eff}} + h.\tan\varphi) \tag{4}$$

The stability margin is directly related to the critical angle. If the critical angle θ_{critital} is substituted into Eq.(3), replacing φ, the SM value equals zero.

$$SM = b - (\chi_{\text{eff}} + h.\tan\theta_{\text{critical}}) = 0 \tag{5}$$

2.3. Structural Analysis based on Finite Element Analysis (FEA)

The final stage involved structural analysis using FEA and optimization analysis to determine the design parameters of the proposed automatic support mechanism. The 3D CAD model created in CATIA was prepared for analysis by removing minor features that did not affect the main load-carrying paths. This reduced the computational load while maintaining the geometry needed for stress prediction. The stand was hinged at the end of the left footrest, and the rider load during mounting and dismounting was applied vertically at the main load-transfer area of the footrest. The von Mises stress distribution and total deformation were used to evaluate the mechanism's structural performance.

A static structural analysis was conducted in ANSYS Workbench to evaluate the automatic stand's strength. Mild steel was modeled as a linear elastic and isotropic material, with an elastic modulus of 200 GPa, Poisson's ratio of 0.30, yield strength of 250 MPa, and density of 7,850 kg/m³. A safety factor of 3 was selected to provide a conservative design margin for uncertainties in loading, material properties, and operating conditions, resulting in an allowable stress of 83.33 MPa.

A load of 981 N, representing the maximum rider mass of 100 kg, was applied at the main load-transfer area of the footrest. Fixed supports were assigned to the stand's ground-contact surfaces. The model was meshed using SOLID187 elements. Mesh convergence was checked by comparing maximum equivalent stress across different mesh sizes. The mesh was considered converged when further refinement produced only a small change in stress. Therefore, an element size of 5 mm was selected, resulting in 6,985 nodes and 3,540 elements. No contact definition was required because the stand was modeled as a single continuous solid body.

2.3.1. Boundary condition

The support and load application during the analysis. In this study, two boundary conditions were defined for the FEA, as shown in Figure 4. A fixed support was applied to the surfaces where the stand connects to the cylinders in contact with the ground. These surfaces were assumed to be fully constrained because they represent the parts of the stand that are held in place and do not move when a load is applied.

The second boundary condition was defined by applying a maximum load to the stand's upper surface to represent the maximum rider weight of 100 kg. By applying both the support constraints and the load in this manner, the stand's structural behavior can be evaluated under the specified loading conditions.

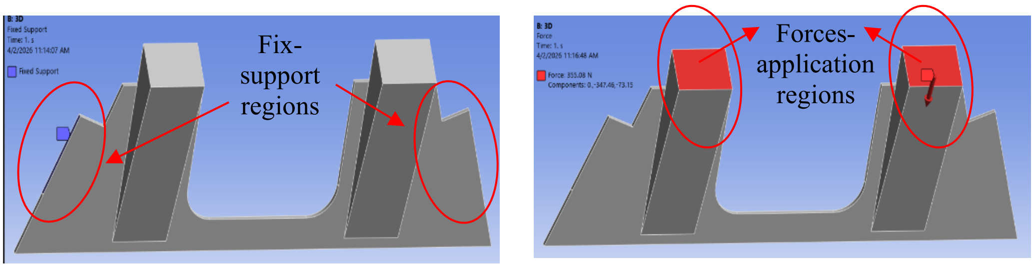

Figure 4. The identification of the boundary conditions: (a) Fixed supports (b) Applied forces

2.3.2. Mesh Sensitivity

Mesh sensitivity analysis examines how mesh size influences the stress results. The model is analyzed with different mesh sizes, producing different numbers of elements and corresponding stress values. These results are plotted as a graph of the number of elements versus the equivalent stress. When the curve begins to flatten, the results are considered to have converged. The mesh size at the start of this convergence region is selected as the optimal mesh size, as it provides stable stress results without unnecessary refinement. This mesh size is then used in the optimization analysis to determine the optimal design parameters.

2.3.3. Optimization

A parameter-based optimization was performed using ANSYS DesignXplorer. The center width and stand-plate thickness were defined as input parameters, while the maximum equivalent stress and stand mass were selected as output parameters. The center width was varied from 40 to 48 mm, and the stand-plate thickness from 2 to 6 mm. The analysis generated 8 design points within these ranges. All other parameters, including the material properties, boundary conditions, and applied load, were kept constant. The optimization aimed to reduce the maximum equivalent stress and stand mass while keeping the stress below the allowable limit of 83.33 MPa.

Among the eight design points, a center width of 43 mm and a plate thickness of 2 mm were selected because they best balanced lower mass with acceptable stress. The final maximum stress was 66.723 MPa, which remained below the allowable limit of 83.33 MPa.

https://doi.org/10.31436/iiumej.v27i3.4618

Therefore, these dimensions represent the best feasible design among the evaluated cases rather than a formally determined global optimum.

2.4. Conceptual Design Development and System Integration

Following the TRIZ analysis and concept selection, the selected Nested Doll principle was translated into a foldable automatic stand mechanism. The stand was designed to remain compact beneath the existing Flexi-UC footrest and deploy only when additional lateral support was required. The conceptual design was developed using CATIA V5, where the mechanical components were modeled, assembled, and integrated with the existing Flexi-UC.

Figure 5 shows the main components of the proposed automatic stand, including the footrest stand, support plate, hinge, actuator link, servo motor, and servo motor casing. The components were modeled and assembled using CATIA V5 and integrated beneath the existing Flexi-UC footrest. This arrangement lets the stand provide extra ground support during mounting and dismounting while remaining compact during riding.

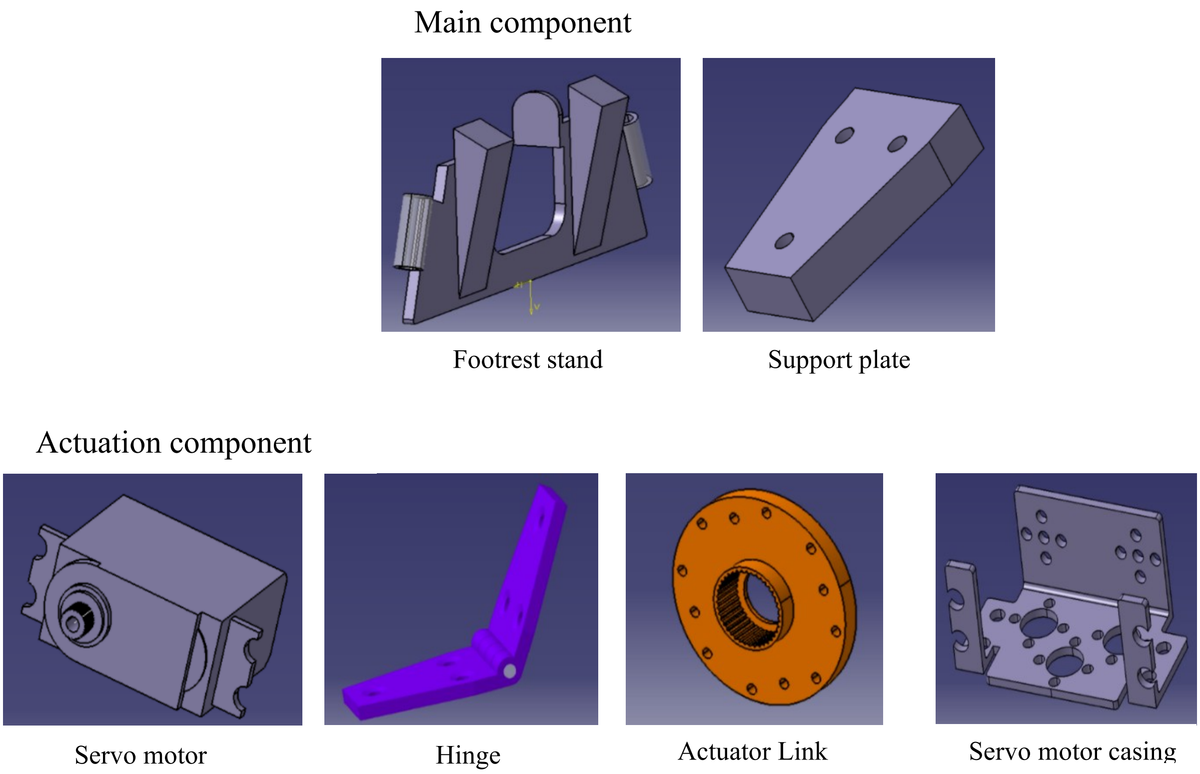

Figure 5. Main mechanical and actuation components of the proposed automatic stand

2.4.1. Automatic Actuation and Control System

The automatic actuation system was developed using an infrared (IR) reflective sensor, an Arduino Uno, and an MG996R servo motor. The IR sensor detected wheel rotation through black-and-white markings on the rotating wheel. The Arduino processed the sensor signal to determine the wheel speed and compared it with the predefined threshold of 0.5 m/s. At speeds of 0.5 m/s or below, the servo deployed the stand to provide lateral support during mounting and dismounting. At speeds above 0.5 m/s, the stand was retracted to prevent ground contact during riding. Separate power supplies were used for the Arduino and the servo motor to minimize voltage drop and electrical noise. Table 4 summarizes the main electrical and electronic components used in the automatic stand system and their respective functions. The components support the sensing, control, actuation, and power supply required for automatic stand operation.

Table 4. Electrical and electronic components of the automatic stand system

No	Component	Function
1	Arduino Uno	Microcontroller that controls the entire system
2	Breadboard	Provides a platform for building circuits without soldering
3	MG996R Servo Motor	Produces rotational motion to actuate the mechanism
4	IR Sensor	Detects objects or movement using infrared signals
5	Step-Down Converter	Converts higher voltage to stable 5V supply
6	Rechargeable Batteries	Supplies electrical power to the system
7	Jumper Wires	Connect electrical components together

3. Results and Discussion

This section discusses the findings and results in relation to the study's objectives. The findings are organized into four sections. The first section presents the TRIZ results, where the identified contradictions and inventive principles lead to the development of the proposed mechanism. The second section presents the theoretical stability analysis using analytical equations to evaluate the improvement in lateral stability. The third section presents the FEA results to evaluate the structural strength and reliability of the proposed design under the applied loading conditions. Finally, the fourth section presents the fabricated conceptual design, in which the automatic stand is integrated at the end of the Flexi-UC footrest to provide additional lateral support during mounting and dismounting. Collectively, these findings provide an overall evaluation of the proposed solution and its capability to improve the lateral stability of the Flexi-UC.

3.1. TRIZ-Based Problem Analysis Result

3.1.1. Function Analysis

The functional analysis after improvement complements the FEA results and supports the conclusion that the additional mechanism can withstand the applied load with adequate structural strength.

After developing the conceptual design, the functional analysis was updated, as shown in Figure 6. The automatic stand introduces an additional ground-support interaction, widening the support polygon and improving lateral stability. It also addresses the previously harmful rider-footrest interaction while retaining the original structure with only one additional subsystem. This minimal modification is consistent with the TRIZ concept of increasing system ideality.

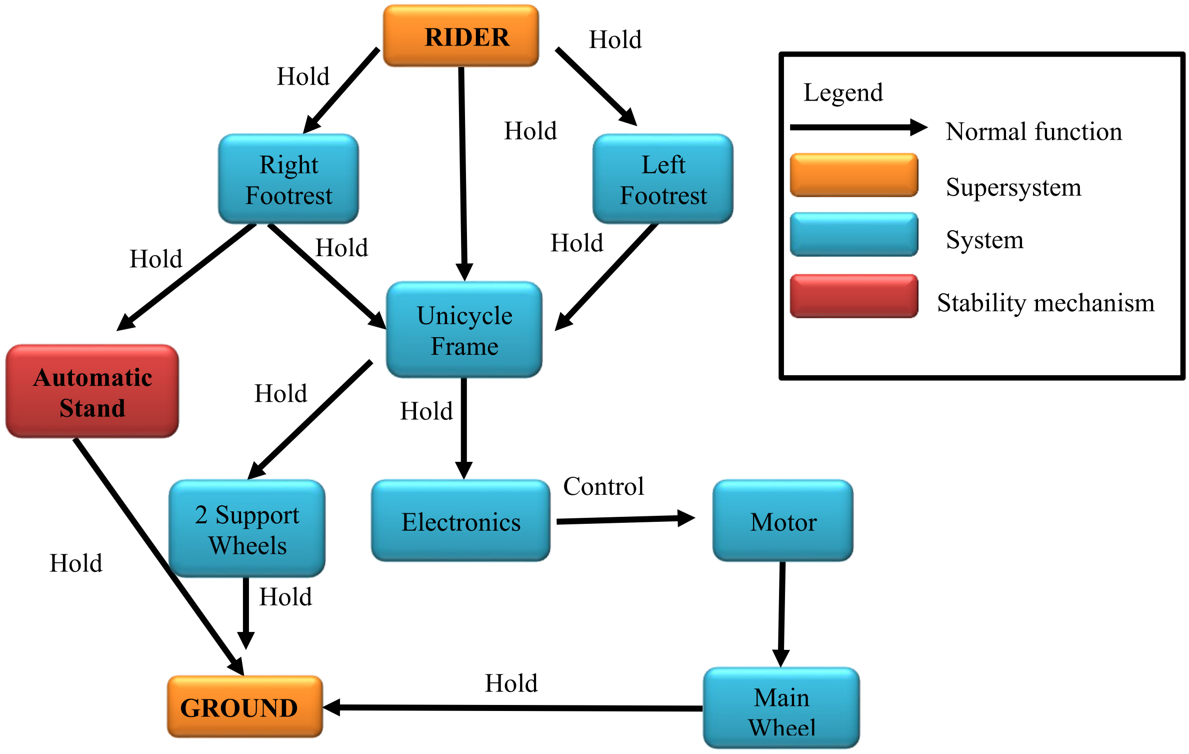

Figure 6. Function Analysis for the research after the improvement

3.1.2. Cause and Effect Chain Analysis (CECA)

The chains used to identify the root causes of Flexi-UC's tendency to topple during mounting and dismounting are shown in Figure 7. The major problem is insufficient contact area between the unicycle and the ground, which reduces available lateral support. Several factors further influence this issue: the limited contact footprint restricts the reaction forces needed for stabilization; the lightweight design with fewer structural components reduces support between the unicycle and the ground; and together, these effects increase the likelihood of toppling when the unicycle is stationary or moving slowly. Collectively, these root causes highlight the need for an auxiliary mechanism that increases ground contact and provides additional support to overcome Flexi-UC instability during mounting, dismounting, and low-speed phases.

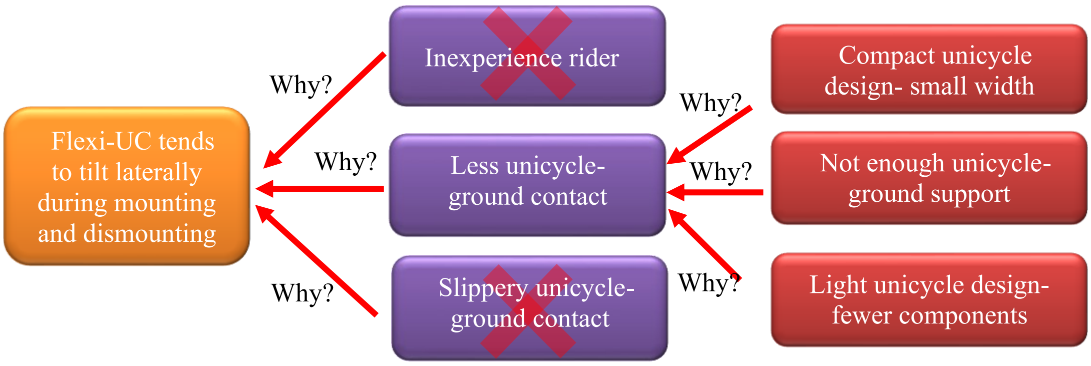

Figure 7. The cause-and-effect chain analysis (CECA)

3.1.3. Engineering Contradiction

Engineering contradiction (EC), also known as a technical contradiction, refers to a situation in which improving one aspect of an engineering system often leads to the degradation of another [19]. In this study, we considered two pairs of engineering contradictions (ECs): the area of the stationary object vs. its length, and the volume of the stationary object vs. its length. Table 5 presents the inventive principles obtained from the contradiction matrix based on the selected contradiction parameters.

Table 5. Extracted from the contradiction matrix [12]

Improving features	Worsening features	Solution from contradiction matrix	
Area of stationary object	Length of stationary object	7 - Nested 9 - Preliminary Anti-Action	26-Copying 39 – Inert atmosphere
Volume of stationary object	Length of stationary object	2 - Taking out 8 - Anti-Weight	14 - Curvature 35 – Parameter changes

Table 6. Relevance analysis of TRIZ inventive principles for Flexi-UC stability enhancement

Principle	Application idea	Relevance	Reasons
26– Copying	Use a simple mock-up or passive stabilizer instead of complex gyroscopic/sensor systems.	×	Doesn't address the core need for additional support during static phases; unsuitable for the project goal.
7 - Nested Doll	**Design a mechanism that folds and stores compactly inside the unicycle's body/frame.**	✓	**Supports the challenge; mechanisms can fold/unfold neatly inside without affecting portability or aesthetics.**
9 - Preliminary Anti-Action	Pre-deploy a stabilizer or footrest before the unicycle stops to prevent toppling.	×	This refers to internal counteractions (like stress) that prevent harm, not a structural/mechanical anti-toppling system.
39 - Inert Atmosphere	Use passive damping materials or inert mechanical elements to reduce vibrations/movement.	×	Focuses on chemical or environmental stability, not on a structural or mechanical stability issue.
35- Parameter Changes	Use materials that change stiffness or shape based on temperature or electric current for a deployable footrest.	×	Material transformation doesn't relate to adding a structural extension to enhance stability.
8. Anti-Weight	Use a lightweight material to keep the unicycle from feeling heavy.	×	Stability is a structural issue, not a weight-based one.
14. Curvature	Design the footrest to curve around the unicycle frame.	×	This principle does not directly address that specific challenge.
2. Taking Out	Eliminate the rider's reliance on body balancing by making the support function a new, separate mechanism.	×	The rider's balance control is self-regulated; it's not a system component that can be removed/isolated by design

Meanwhile, Table 6 shows the assessment of inventive principles based on the TRIZ contradiction matrix to enhance the Flexi-UC's lateral stability. The principles were evaluated separately for relevance, practicability, and appropriateness to the project objectives, focusing on increased stability during mounting and dismounting while maintaining a compact installation size. Most of the proposed principles were less suitable because they did not directly address the need for structural stability during mounting and dismounting. Among the evaluated principles, only Principle 7, Nested Doll, was identified as directly applicable. The principle led to the idea of a foldable and retractable footrest stand that can be stored within the unicycle frame when not in use and deployed when needed, addressing the need for greater stability while overcoming space limitations. The other principles, although novel in other contexts, were less suitable because they primarily involve material modification, environmental effects, redistribution of internal forces, or weight minimization, none of which directly enhances mechanical stability in this case. One principle was also considered impractical because the rider controls balance and cannot regulate it externally through mechanical means. As a result, the Nested Doll principle emerged as the most appropriate conceptual basis for the automatic footrest stand, as it enables a compact yet deployable stabilization system while retaining the unicycle's overall functionality and design integrity.

3.1.4. Physical Contradictions

Physical contradictions (PCs) refer to opposite requirements for a design parameter within the same system [13]. The paradox of the existing Flexi-UC design is that a large ground-contact area is needed during mounting and dismounting to maintain lateral stability, while a small contact area is required during riding to reduce interference.. The improved Flexi-UC addresses this contradiction by applying TRIZ Separation in Time and Separation upon Condition, so the stand deploys only during mounting and dismounting and remains compact during riding. This technical paradox can be resolved using appropriate TRIZ tools, such as the separation principles for physical contradiction.

Table 7. The physical contradiction involved

Element Involved	Conflicting Requirements
Length and area of contact between unicycle and ground	Needs to be large for stable ground contact and small for compactness

The first step in a physical contradiction analysis is to identify the element involved and to explain the conflicting requirements. In this case, as shown in Table 7, the conflict is between the unicycle's size and its ground contact area. A larger contact area improves stability when the unicycle is static, but keeping the unicycle small and compact reduces that area. In other words, the contact area or length must be both large and small at the same time. To resolve these conflicting requirements, TRIZ provides four separation principles: Separation in Time, Separation in Space, Separation upon Condition, and Separation between Whole and Parts [13].

A relevance analysis, shown in Table 8, revealed that the most applicable principles are Separation in Time and Separation upon Condition, meaning the footrest stand can be deployed when needed and retracted when not. This approach increases stability without compromising the unicycle's compactness. However, Separation in Space and Separation between Whole and Parts were less applicable because these principles increase design complexity.

Subsequently, Table 9 presents the TRIZ-based resolution strategies derived from these separations. Two key problems were identified: (1) insufficient ground contact during mounting and dismounting, and (2) a bulky stand design that disrupts dynamic motion. To address these, we applied two separation strategies. In time separation, the stand deploys when stationary and retracts during motion, ensuring both stability and compactness. In condition separation, the stand activates only below a threshold speed, making it responsive to real-time riding conditions. Together, these strategies keep the footrest compact when not in use and deploy it automatically when needed, improving stability without compromising maneuverability.

Table 8. Relevance of TRIZ separation concepts in addressing the physical contradiction

Type of separation	Contradiction Element	Application Idea in the project	Relevant to Project?	Reasons
Separation in Time	Contact ground area must be small for compactness and large for stability	**Keep unicycle compact; footrest unfolds for lateral support**	**✓ Relevant**	**Unfolds only when needed**
Separation in Condition		**Compact design: parts extend temporarily for support**	**✓ Relevant**	**Depends on speed/rider input**
Separation in Space		Not applicable	✗ Irrelevant	Increase design complexity
Separation between whole and parts		Not applicable	✗ Irrelevant	Increase design complexity

Table 9. The physical contradiction and TRIZ-based solution

Types of separation	TRIZ-based solution	
In time i. The stand is deployed only when stationary, and retracted during motion. *In condition* i. The stand activates only when the speed falls below a threshold of 0.5 m/s.	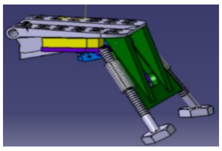 Deployed during mounting and dismounting phase.	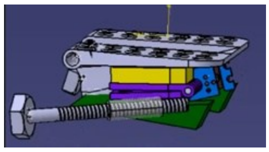 Neatly installed under footrest.

Although the control system prevents commanded deployment above 0.5 m/s, an operational safety response was considered. If the stand fails to deploy, the rider can move slowly towards a level stopping area or nearby fixed support before dismounting. If unintended deployment occurs during riding, the stand remains above the ground and does not immediately interfere with wheel movement. The rider can then reduce the speed, stop on a level surface, and dismount safely. Therefore, these failure conditions do not immediately compromise rider safety.

3.2. Stability Analysis Using Analytical Equations

A preliminary static stability analysis was conducted to verify improved lateral stability. This evaluation provides a simple yet quantitative measure of how the proposed foldable footrest stand influences the unicycle's resistance to toppling. A comparison of the support polygon width and center of gravity (CoG) projection under three conditions, namely mounting the Flexi-UC with the stand, mounting without the stand, and riding the Flexi-UC, is presented in Table 8. *P* denotes the weight of the rider, *W* is the weight of the Flexi-UC, *b* is the distance at which the Flexi-UC contacts the ground, and e_1 to be denoted as the distance between the center of the *b* and *P* while e_2 is the distance between the center of *b* and *W*.

To clarify the diagram in Table 10, the purple line represents the Center of Gravity (CoG) of the rider, P, while the red dashed line represents the CoG of the Flexi-UC, W. The green line indicates the center of the base width, and the blue dashed lines indicate the stability boundaries of the base. During mounting and dismounting with the stand deployed, the base width increases to 34.5 cm, keeping the CoG projection within the stability boundary. This provides greater lateral stability and makes mounting and dismounting easier and safer. Without stand

https://doi.org/10.31436/iiumej.v27i3.4618

deployment, the base width is only 11.5 cm, causing the CoG projection to fall outside the stability boundary. This creates an unstable condition and increases the likelihood that the Flexi-UC will tip sideways. During riding, when both feet are in full contact with the footrests, the base width is 23 cm, and the CoG projection remains within the stability boundary, which is sufficient to maintain lateral stability.

Table 10. Comparison of support polygon and CoG projection in three conditions

Condition		Support polygon and CoG projection (P+W)	
Mounting and dismounting Without stand	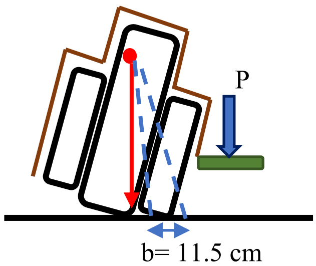	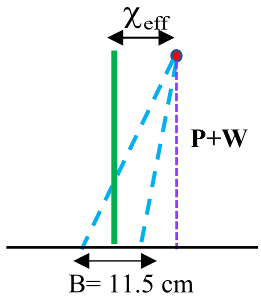	The base width is narrow, the projected CoG is already outside the boundary.
Mounting and dismounting with stand	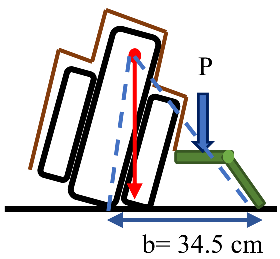	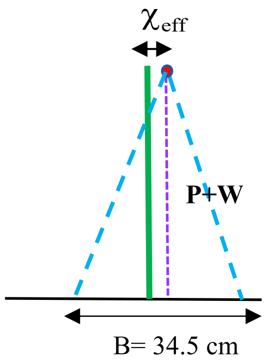	The base width is wider, and the center of the width shifted to the right
Normal riding	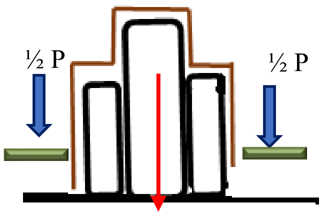	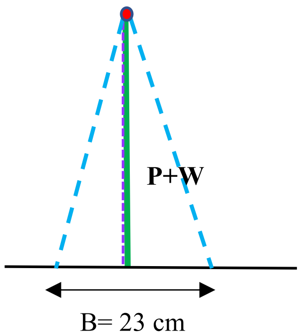	The system's CoG is aligned with the centre of the support base.

Indicators:

Centre of Gravity of Flexi UC and rider

Centre of the base width

Stability boundary (length of the base)

3.2.1. Lateral CoG displacement.

Lateral CoG displacement is the effective lateral displacement of the center of gravity (CoG) of the unicycle. All computations used a typical rider weight of 70 kg and a unicycle weight of 25 kg, standard values in the stability literature representing an average adult and a mid-weight EUC. The effective lateral CoG displacement and the vertical CoG displacement h_{eff} of the combined rider–unicycle system are approximated using a mass-weighted average of the individual lateral CoG positions, assuming quasi-static conditions and a centrally aligned unicycle CoG. When g = 9.81 m/s^2, the weight of the rider is P = 686.7 N, and the weight of the unicycle is W = 245.25 N. e_1 is the distance between the CoG of the Flexi UC and the center of the width base, while e_2 is the distance between the CoG of the rider and the center of the width base. For the without-stand condition, e_1 is -1.305 cm, while e_2 is 19.05 cm, and for the with-stand condition, e_1 is 12.27 cm, while e_2 is 8.1 cm. Meanwhile h_1 and h_2 are the individual CoG heights for the Flexi-UC and the rider, respectively. When the stand is deployed, the support base is not displaced; it is only spread out. Therefore, the collective offset in the lateral CoG is solely dependent on P, and W will remain identical with or without the stand. Consequently, the formula for lateral CoG displacement. Equation (4) and vertical CoG displacement, h_{eff}; using the adaptation of the formula introduced by Rahman [20] will give:

$$\chi_{\text{eff}} = \frac{W.e_1 + P.e_2}{W + P} \tag{6}$$

$$h_{\text{eff}} = \frac{W.h_1 + P.h_2}{W + P} \tag{7}$$

χ_{eff} are calculated separately in both cases: without stand and with stand, where the value of e is different for both cases.

χ_{eff} without stand:

$$\chi_{\text{eff1}} = \frac{245.25(-0.01305) + 686.7(0.1905)}{245.25 + 686.7} = 0.1368 \text{ m} \tag{8}$$

χ_{eff} with stand:

$$\chi_{\text{eff2}} = \frac{245.25(-0.1227) + 686.7(0.081)}{245.25 + 686.7} = 0.0274 \text{ m} \tag{9}$$

While for h_{eff} is the same for both cases.

$$h_{\text{eff}} = \frac{W.h_1 + P.h_2}{W + P} = \frac{245.25(0.2) + 686.7(0.95)}{245.25 + 686.7} = 0.753 \text{ m} \tag{10}$$

The values of the and h_{eff} above are used to calculate the critical angle and SM.

a. <u>Critical angle during mounting and dismounting with stand</u>:

The value from equation (2) will be substituted into equation (5), which will give

$$\theta_{\text{critical}} = \tan^{-1}\left(\frac{b - \chi_{\text{eff2}}}{h_{\text{eff2}}}\right) => \tan^{-1}\left(\frac{0.1725 - 0.0274}{0.7527}\right) = 10.9^0 \tag{11}$$

When the stand is deployed, the base width of the unicycle increases substantially, and the critical toppling angle increases to 10.9°. This shows that the system can tolerate a larger sideways lean before tipping over, representing a substantial improvement compared with the condition without stand deployment. Although the unicycle reaches its critical angle at 10.9°, the rider can still maintain balance because the critical lean angle for a standing human is about 17.7° [21]. This is comparable to standing on a stationary four-wheel skateboard or climbing a V-shaped ladder, where the toppling angle is around 10°. These situations suggest that a person can maintain balance under similar static conditions. As a result, the stand helps keep the unicycle upright and stable during mounting and dismounting, similar to the situations described above.

b. Critical angle during mounting and dismounting without stand:

$$\theta_{\text{critital}} = \tan^{-1}\left(\frac{b-\chi_{\text{eff1}}}{h_{\text{eff1}}}\right) => \tan^{-1}\left(\frac{0.0575-0.1368}{0.7527}\right) = -6.01^{0} \tag{12}$$

The small critical angle indicates that the human–unicycle system is near the limit of static stability at rest, even in the absence of additional external disturbances, since the effective center of gravity lies very close to the edge of the base. The sign of the critical angle indicates the direction of lean, while its magnitude of 6.01° represents the onset of lateral instability. Under this condition, the unicycle cannot remain steady on its own without external support, as even minor disturbances may cause the center of gravity projection to move beyond the support boundary. This finding indicates that toppling can be induced by very slight lateral movement without a stand or other external support. It highlights the inherent instability first-time riders encounter during mounting and dismounting, when maintaining balance is difficult unless additional structural support is provided.

c. Critical angle during riding:

$$\theta_{\text{critital}} = \tan^{-1}\left(\frac{b-\chi_{\text{eff}}}{h_{\text{eff}}}\right) => \tan^{-1}\left(\frac{0.115}{0.753}\right) = 8.7^{0} \tag{13}$$

The lateral load of the rider is symmetrically distributed between both footrests during riding while the stand remains fully retracted; therefore, there is no distinction between riding with or without the stand, and the effective lateral CoG offset is nearly zero $\chi_{\text{eff}} \approx 0^{0}$. The width of the unicycle with the footrests unfolded defines the support base, while the stand width does not contribute to stability when it is folded. This positive angle suggests that, when riding straight with the CoG centered, the CoG projection remains well within the support base over a relatively large lean range, with the theoretical stability limit reached when the lean exceeds 8.7°. In practice, the achievable lean before loss of control may be lower due to additional dynamic constraints such as main wheel grip, surface irregularities, and rider control. During riding, small steering corrections and the gyroscopic effects of the moving wheel also support balance. Thus, this value provides a reference point for why riding is more stable than mounting and dismounting.

Overall, the critical angle analysis shows a clear difference among the three operating conditions. Without the stand, the system's critical angle during mounting and dismounting is very low at −6.01°, indicating that the system is near the stability limit and can be easily disturbed by minor lateral movements. When the stand is deployed, the support base widens, and the tipping threshold shifts outward, with the critical angle increasing to approximately 10.9°, providing a greater stability margin during weight transfer in mounting and dismounting. During riding, the critical angle is 8.7°, indicating sufficient stability for forward motion, with the rider and dynamic effects largely maintaining balance. These findings demonstrate that the stand enhances lateral stability in slow or near-static conditions, particularly during mounting and dismounting, without adversely affecting stability during riding.

Table 11. Comparison of critical angle for unicycle with stand and without stand while mounting and dismounting, and in addition during riding

Condition	Critical angle (Theoretical)
Mounting and dismounting with stand	10.9^0
Mounting and dismounting without stand	-6.01^0
During riding	8.7^0

Table 11 shows that the stand plays an important role in improving lateral stability during mounting and dismounting. The stand's enlarged support polygon keeps the CoG projection well within the base, providing greater rider stability. Conversely, without the stand, the support base is very narrow, and the CoG projection is near the edge of the support polygon. This condition makes the unicycle highly sensitive to minor lateral disturbances, which explains why balancing becomes difficult during mounting and dismounting. Once the rider has both feet on the footrests during riding, however, the effective base width increases. In this riding condition, the CoG projection remains within the support polygon, and adequate stability is maintained; thus, the stand becomes less critical.

3.2.2. Stability Margin (SM)

A positive SM indicates that the CoG projection lies within the support base, signifying a stable condition, while a negative SM indicates that the CoG projection has exceeded the boundary, leading to instability. In this way, χ_{eff} from Equation (4) represents the shifted position of the CoG due to mounting, while $h\tan\theta$ accounts for further displacement due to leaning, and SM quantifies the remaining margin before tipping occurs. Selected lean angles are presented as representative low-angle conditions to illustrate the influence of lean angle on the stability margin. We calculated the stability margins by substituting the base width b from Table 10 into Equation (4), and present the results in Table 12.

From Table 12 and Figure 8, the three conditions differ in stability margins. In the upright posture, the system is already unstable with SM = −0.079 m at 0°, and when leaning, the system becomes more unstable with SM = −0.185 m at 8°, indicating that the projection of the CoG is outside the support base and that the unicycle is susceptible to toppling during mounting or dismounting.

Table 12. Comparison of stability margin (SM) at selected lean angles for Flexi-UC with stand and without stand

Lean Angle φ	SM without stand	SM with stand	SM during riding
0^0	-0.079	0.145	0.088
2^0	-0.106	0.119	0.061
5^0	-0.145	0.079	0.022
8	-0.185	0.039	-0.018

The tipping boundary shifts outward when the stand is deployed, resulting in a large positive margin: SM = 0.145 m at 0° and SM = 0.039 m at 8°. This indicates that the CoG projection remains within the support polygon over the tested lean range, providing greater stability during mounting and dismounting. The system is therefore unstable during unsupported mounting and dismounting unless additional support is provided. However, after deploying the automatic stand, the support base widens, shifting the tipping boundary further outward and creating a consistently positive stability margin, thereby providing greater stability during mounting and dismounting. This enhancement shows that the optimized Flexi-UC provides higher static stability than the baseline configuration without the stand.

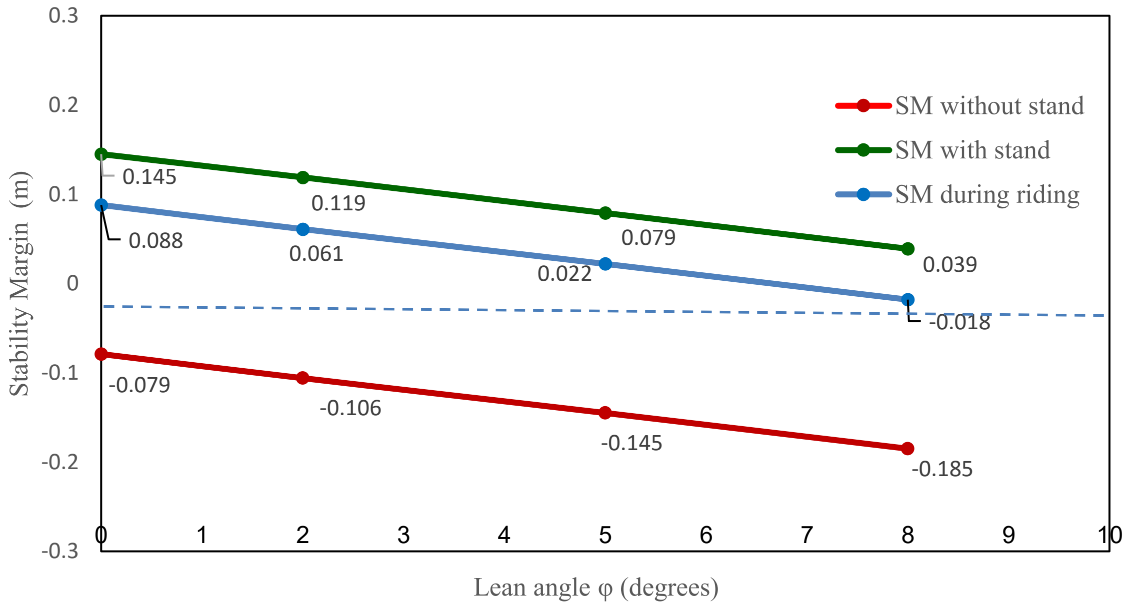

Figure 8. Comparison of stability margin (SM) versus lean angle for three operating phases

During riding, when the stand is folded, the base configuration is positively stable at the lower lean angles tested, where SM = 0.088 m at 0° and decreases to 0.061 m at 2°. However, the stability margin decreases as the lean angle increases and becomes negative at higher angles, with SM = −0.018 m at 8°. This tendency shows that active rider control and dynamic balance become increasingly important in maintaining balance at higher lean angles or under external disturbances. Overall, the results showed that the stand played a major role in improving static stability during mounting and dismounting.

The derived analytical formula verified the relationship between the stability margin and the critical angle. From Equation (3), substituting the critical angle for the lean angle results in SM = 0, corresponding to the zero-crossing points of the stability margin curves. The lean angles at which SM = 0 are very similar to the calculated critical angles for all configurations, demonstrating the internal consistency of the static stability model and supporting the validity of the adopted formulation.

3.3. Structural Analysis Using Finite Element Analysis (FEA)

FEA was undertaken to determine the structural behavior of the automatic stand mechanism. Because the stand must bear the applied load during mounting and dismounting, a design load of 100 kg, representing the maximum rider mass, was considered. Static loading was considered sufficient because mounting and dismounting occur under stationary or very low-speed conditions and do not require a complex dynamic simulation. It is necessary to ensure that the added structure does not deform beyond acceptable limits and that stress concentrations remain within allowable limits. The analysis was based on three criteria: total deformation to assess the stiffness and geometric stability of the stand; von Mises stress to verify that the maximum stress remains below the allowable stress of mild steel after applying a safety factor of 3, which is 83.33 MPa; and design optimization to reduce the overall mass of the component without adversely affecting performance. A safety factor of 3 was used in this design. This value is supported in the literature, where a safety factor of 3 has been used in tubular space-frame chassis designs to ensure structural safety under high loading conditions. Therefore, a safety factor of 3 was considered suitable for the proposed structural component [22].

3.3.1. Mesh sensitivity

Before optimization, a mesh sensitivity analysis was conducted to determine a suitable mesh size for the subsequent optimization analysis. Figure 9 shows a sensitivity graph of maximum stress convergence versus the number of elements. From the graph, the stress values begin to converge at 3,522 elements, corresponding to a mesh size of 5 mm. Therefore, this mesh size was selected for the optimization analysis.

A mesh convergence study was conducted using element sizes of 20, 13, 10, 6, 5, 4, 3, and 3.5 mm. The maximum equivalent stress values obtained for each mesh were 7.021, 10.24, and 10.63 MPa, respectively. Mesh convergence was considered achieved when the difference in maximum equivalent stress between two successive mesh refinements was below 5%. Therefore, the final analysis used an element size of 5 mm.

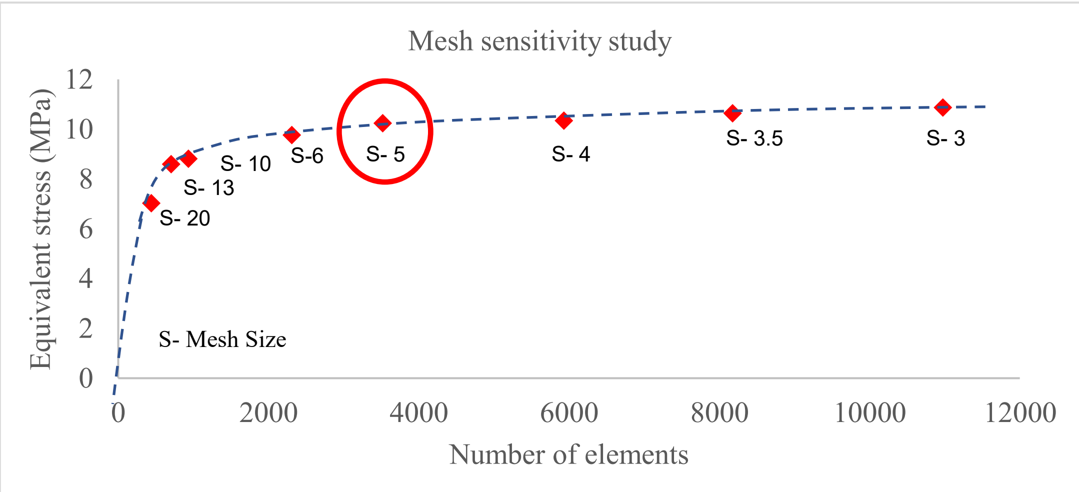

Figure 9. Mesh sensitivity graph of Equivalent Stress vs. Number of elements

3.3.2. Optimization

For this design, two parameters were considered as independent variables: the center width and the thickness of the stand plate, as shown in Figure 10. The dependent variables are the maximum stress in the stand under the maximum applied load and the stand weight. Other parameters were treated as controlled variables.

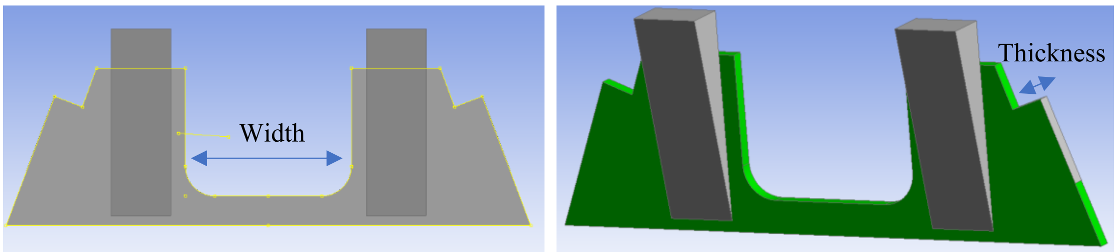

Figure 10. Input parameters used in the ANSYS DesignXplorer optimization

Based on the evaluated design points, the analysis identified a center width of 43 mm and a plate thickness of 2 mm as the most suitable combination within the specified parameter ranges. This configuration produced a stand mass of 0.6 kg and a maximum equivalent stress of 66.723 MPa under a static load equivalent to a 100 kg rider.

Since the maximum stress remained below the allowable stress of 83.33 MPa, the selected geometry was considered structurally safe. The configuration also maintained a compact and lightweight design suitable for integration with the Flexi-UC footrest. The selected dimensions represent the most suitable design identified within the evaluated parameter ranges rather than a global optimum. Overall, the selected geometry can safely support the maximum design load of 100 kg, representing the maximum rider mass, while minimizing unnecessary material use. The final design is structurally adequate, compact, and suitable as a lateral stabilizing mechanism for the improved Flexi-UC system.

3.3.3. Total deformation

The maximum total deformation of the automatic stand was 0.363 mm at the lower part of the stand, as shown in Figure 11. This displacement is very small compared with the component's overall size, indicating that the structure maintains geometric stability under the applied load. The minimal bending also confirms that the stand is sufficiently stiff to remain dimensionally stable during rider mounting and dismounting, with only minimal changes to the support geometry. These results confirm that the stand maintains sufficient structural rigidity and is structurally viable under the intended operating conditions.

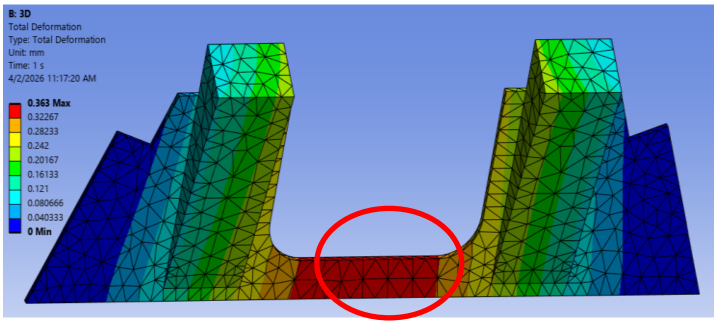

Figure 11. Total deformation contour of the optimized design

3.3.4. Equivalent Stress

Figure 12 shows the von Mises stress distribution of the automatic stand, with a maximum stress of 66.723 MPa, which is approximately 80.1% of the allowable stress of 83.33 MPa. These results confirm that the automatic stand does not exhibit critical stress concentrations exceeding the allowable limit and is structurally suitable for mounting and dismounting under the specified static loading conditions.

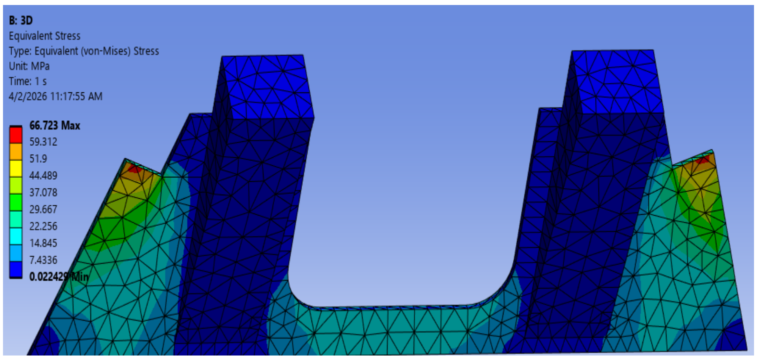

Figure 12. Equivalent Von Mises stress distribution of the optimized component

3.4. Conceptual Design and Prototype Integration

The final conceptual design was developed based on the selected TRIZ solution. Figure 13 shows the final CAD assembly and fabricated prototype of the automatic footrest stand. The mechanism was then integrated with the existing Flexi-UC, as shown in Figure 14. The stand was positioned beneath the footrest to provide additional lateral ground support during mounting and dismounting while maintaining compactness when retracted.

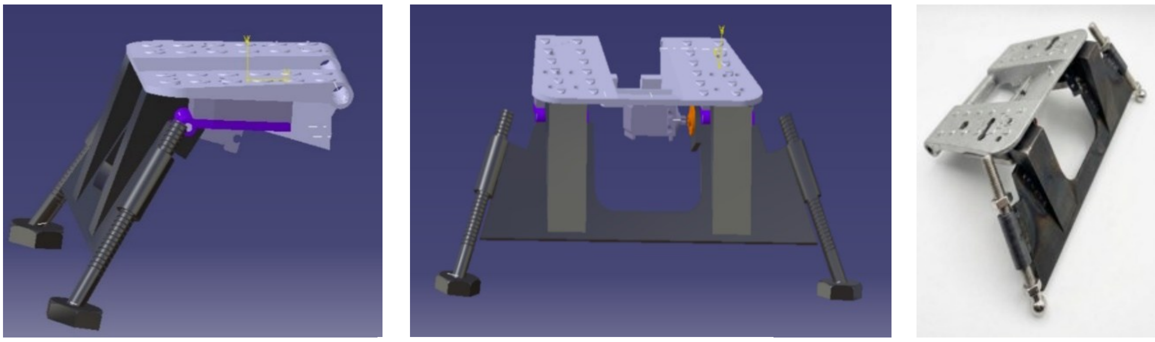

CAD assembly – Side view CAD assembly – Front view Actual

Figure 13. Final automatic footrest stand: CAD model and fabricated prototype

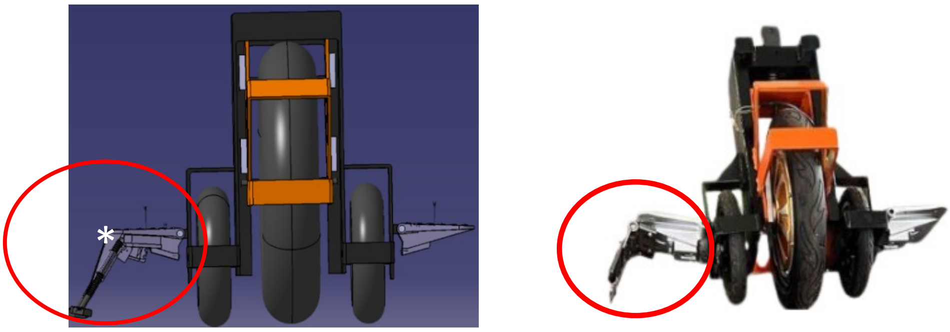

CAD assembly Actual prototype

Figure 14. Integration of the automatic footrest stand with the Flexi-UC

The automatic stand added to the Flexi-UC, as shown in Figure 14, provides additional lateral support during mounting and dismounting and retracts during riding to keep the unicycle compact and prevent interference with the rider's movement. The FEA results confirm that the maximum stress remains below the allowable limit and that the design's total deformation is minimal. The improved functional analysis was subsequently refined to reflect the Engineering Contradiction (EC), Physical Contradiction (PC), and the validated performance of the optimized design. The mechanical integrity demonstrated by the simulations supports including the automatic stand as a stabilizing subsystem, indicating that the proposed mechanism can provide the intended ground-contact function without compromising the design's compactness. With the contradictions resolved, the updated functional analysis shows how the automatic stand integrates into the system as a functional stabilizing element.

Overall, Table 13 summarizes the key features of the Flexi-UC before and after the improvement. This comparison clearly shows how the improved Flexi-UC addresses the earlier design problem, with the added support function improving stability and overall system performance.

https://doi.org/10.31436/iiumej.v27i3.4618

Table 13. The comparison table for before improvement and after improvement

Feature	Before Improvement	After Improvement
Stability mechanism	Entirely on the rider	Rider + mechanical stand support
Footrest role	Passive platform	Interface for stand activation (indirect)
Ground interaction	2 points (main wheel and one support wheel)	3 points (main wheel + 1 support wheel + stand)
Sensitivity to supersystem	High	Reduced
System ideality	Lower	Higher due to added passive function

4. CONCLUSION

The lateral stability issue during mounting and dismounting of EUCs has received little attention, and this paper addresses it systematically through the TRIZ method. This issue was addressed through an inventive solution developed using functional analysis, cause-and-effect chain analysis (CECA), engineering contradiction, and physical contradiction to conceptualize an innovative mechanism to overcome the main problem. This added mechanism does not compromise the Flexi-UC's compactness or riding dynamics. The TRIZ-guided design process helped resolve major physical contradictions and led to the development of an additional mechanism, namely the automatic stand, thereby improving the existing Flexi-UC design. The stability analysis indicated that the stability margin improved substantially and that the theoretical critical angle increased from −6.01° to 10.9°, while the stability margin increased from a negative value of approximately −0.08 m to a positive value of about +0.15 m under the stand-deployed condition. The finite element analysis confirmed that the structure operates safely within the elastic range with minimal deformation under the applied load, supporting the proposed mechanism's structural integrity.

The results indicate that TRIZ offers a systematic approach to converting design contradictions into practical engineering solutions, leading to a compact and reliable Flexi-UC mechanism that increases lateral stability, particularly during mounting and dismounting, while also contributing to innovation in micromobility design. Further experiments can be conducted with users under riding conditions to evaluate the mechanism's robustness, ergonomic comfort, and long-term durability. Future work should focus on improving the control logic and actuation responsiveness while minimizing the impact on battery performance. Dynamic, fatigue, and impact testing under cyclic loading conditions are recommended to evaluate the automatic stand’s long-term structural durability. Future work should include dynamic and impact loading, along with fatigue and cyclic testing, to assess the automatic stand's long-term durability. The actuation system can also be improved in response and reliability. Consider an independent mechanical fail-safe or interlocking mechanism to prevent unintended stand deployment during riding. Further improvement should also focus on reducing the overall system mass. Testing with a larger and more diverse group of participants is recommended to provide a broader evaluation of the proposed design’s usability and ergonomic performance. Overall, this research shows that TRIZ can be used as a systematic approach to produce practical design improvements and solve engineering problems in future personal mobility systems.

ACKNOWLEDGMENT

The authors gratefully acknowledge their respective institutions for their strong support in this study. All authors consent to the publication of this manuscript**.**

REFERENCES

[1] M. Gonçalves and P. Cash, "The life cycle of creative ideas: Towards a dual-process theory of ideation," *Des. Stud.*, vol. 72, Jan. 2021, https://doi.org/10.1016/j.destud.2020.100988 .

[2] L. Chechurin, "TRIZ in Science. Reviewing Indexed Publications," in *Procedia CIRP*, Elsevier B.V., 2016, pp. 156–165 . https://doi.org/10.1016/j.procir.2016.01.182 .

[3] P. Cuffe, "Flexible Mobility in the Smart City: The Role of Small Personal Electric Vehicles Flexible mobility in the smart city," *DIT – eseia Conference on Smart Energy Systems in Cities and Regions, Dublin, Irelan*, pp. 10–12, Feb. 2018, [Online]. Available: http://hdl.handle.net/10197/9938

[4] D. Reyes-Huerta, H. Mitre-Hernandez, and U. Jaramillo-Avila, "Teaching and Learning TRIZ as an Innovative Educational Technology: A Systematic Literature Review," 2023.

[5] O. Şen, "An Implementation of TRIZ in Innovative Product Development: An Oil Cap for Propeller Shaft," *Sakarya University Journal of Science*, vol. 28, no. 6, pp. 1296–1306, Dec. 2024, https://doi.org/10.16984/saufenbilder.1514093

[6] N. Ramli, M. A. Azizi, N. A. Aziz, and M. A. Azman, "Advances and challenges in electric unicycle stability: a review of structural design and control mechanisms," *Journal of Engineering and Applied Science*, vol. 72, no. 1, p. 197, Dec. 2025, https://doi.org/10.1186/s44147-025-00778-7

[7] Travers *et al.*, "Moral Panic and Electric Micromobilities: Seeking Space for Mobility Justice," *Sociological Perspectives*, vol. 67, no. 1–3, pp. 83–108, Jun. 2024, doi: https://doi.org/10.1177/07311214231193355

[8] L. Mihályi, X. A. Ji, G. Orosz, and D. Takács, "Data Collection for Learning the Dynamics and Control of an Electric Unicycle," *The Evolving Scholar*, 2023, https://doi.org/10.24404/63fdc92b57f7d2ada3a24289

[9] Kang FK, "Stabilized electric unicycle, Flexi UC fabrication and experimental.," Universiti Putra Malaysia, 2024.

[10] INMOTION USA, "InMotion V11 Electric Unicycle," INMOTION USA. [Online]. Available: https://www.myinmotion.com/products/inmotion-v11-electric-unicycle. [Accessed: Aug. 6, 2026].

[11] Zuo, G. (2018). Intelligent somatic full-balance electric vehicle (U.S. Patent No. 9,908,579 B2). United States Patent and Trademark Office. https://patents.google.com/patent/US9908579B2/en

[12] T. S. Yeoh, T. J. Yeoh, and C. L. Song, *TRIZ Systematic Innovation in Manufacturing*, 11th ed., vol. 1. Malaysia: Firstfruits Sdn Bhd, 2009.

[13] K. Szczepanik and J. A. Chudziak, "TRIZ Agents: A Multi-Agent LLM Approach for TRIZ-Based Innovation," in *International Conference on Agents and Artificial Intelligence*, Science and Technology Publications, Lda, 2025, pp. 196–207. https://doi.org/10.5220/0013321900003890 .

[14] Scott, N., & Travers, N. (2023). E-micromobility, cycling, and 'good' active travel. Active Travel Studies, 3(1). https://doi.org/10.16997/ats.1206

[15] L. Chen, Y. Song, S. Ding, L. Sun, P. Childs, and H. Zuo, "TRIZ-GPT: An LLM-augmented method for problem-solving," Aug. 2024, [Online]. Available: http://arxiv.org/abs/2408.05897

[16] Su, Y., Ding, L., Xu, P., Wang, G., Wei, Q., Liu, T., Wang, H., & Gao, H. (2025). Dimensional design method based on stability analysis to enhance traversability of heavy-duty hexapod robots over challenging terrains. Mechanism and Machine Theory, 214, 106141. https://doi.org/10.1016/j.mechmachtheory.2025.106141

[17] Mungan, C. E., & Kabutz, H. (2024). The driven unicycle. Physics Education, 59(3), 035026. https://doi.org/10.1088/1361-6552/ad3cc5

[18] Morales, J., Martínez, J. L., Mandow, A., Serón, J., & García-Cerezo, A. J. (2013). Static tip-over stability analysis for a robotic vehicle with a single-axle trailer on slopes based on altered

supporting polygons. IEEE/ASME Transactions on Mechatronics, 18(2), 697–705. https://doi.org/10.1109/TMECH.2011.2181955

[19] Santoso, G., Ammarullah, M. I., Sugiharto, S., Hidayat, T., Khoeron, S., Bayuseno, A. P., & Jamari, J. (2024). TRIZ-based method for developing a conceptual laparoscopic surgeon's chair. Cogent Engineering, 11(1), 2298786. https://doi.org/10.1080/23311916.2023.2298786

[20] Rahman, M. T. A., Ahmad, S., Akmeliawati, R., Altalmas, T., & Aula, A. (2013). Centre of gravity (C.O.G.)-based analysis on the dynamics of the extendable double-link two-wheeled mobile robot. IOP Conference Series: Materials Science and Engineering, 53(1), 012079. https://doi.org/10.1088/1757-899X/53/1/012079

[21] Egoyan, A., & Moistsrapishvili, K. (2013). Equilibrium and stability of the upright human body. General Science Journal, 1–10.
https://www.gsjournal.net/Science Journals/Research%20Papers/View/4581

[22] C. K. Anil, S. Srinivas, M. Manjunath, M. Satish, and M. B. Khot, "Selection of Materials, Design and Analysis of FSAE Chassis for Different Engineering Application- A Comprehensive Review," Mar. 31, 2025, *Society of Automotive Engineers Turkey*. https://doi.org/10.30939/ijastech..1574611 .